ON THE APPLICATION OF BEAMFORMING IN LDACS

Ayten Gürbüz, Daniel M. Mielke, and Miguel A. Bellido-Manganell
German Aerospace Center (DLR), Wessling, Germany

Abstract

Currently, aeronautical communications is undergoing a modernization process from analog to digital technology. The L-band Digital Aeronautical Communications System (LDACS) is the upcoming digital data link for air-ground communications and is being standardized within ICAO as well as EUROCAE at the moment. A wireless communication system can be interrupted by intended or unintended jamming signals. Therefore, the robustness of wireless systems is crucial. In this paper, we investigate the use of beamforming in LDACS to improve its performance and robustness. We analyze different antenna array designs and assess their performance to find the most suitable configuration for LDACS. Accordingly, the chosen antenna array design is evaluated for different flight scenarios considering a realistic LDACS link budget. We show that the chosen phased antenna array design improves the signal-to-noise-ratio of the LDACS reverse link by over 10 dB. Hence, using beamforming, the robustness of LDACS can be enhanced and higher data rates can be achieved by applying the built-in LDACS adaptive coding and modulation capabilities.

Introduction

Global standardized air traffic management (ATM) systems manage all aircraft in controlled airspace to ensure efficient traffic flows and safety of flight. The current ATM works properly; however, the demand for air transportation is continuously growing. The increasing number of flights is a challenge and the current ATM systems are expected to reach their capacity in some world regions within the coming years [1]. To ensure sustainable growth and safety of air transportation, the air-ground (A/G) infrastructure is undergoing modernization [2], [3]. Accordingly, the very high-frequency (VHF) analog air-ground communication system as well as the VHF Date Link Mode 2 (VDL Mode 2) are expected to complemented by LDACS in the coming years [4].

Wireless communication systems are vulnerable to attacks and interferences caused by other operating systems. Therefore, the robustness of the ATM operations is crucial for the systems supporting the safety of life applications. According to the OSI layer model, a digital communication system can be split into multiple layers with different functionalities where each layer depends on its underlying layers. The physical layer is the bottom layer. If the physical layer is disrupted, data transmission is not possible regardless of the security implemented in the upper layers [5].

One technique to increase the physical layer's robustness is beamforming. Beamforming is a method for adjusting the antenna radiation pattern. It can be used to increase the signal power to the chosen direction and reduce the antenna gain to other directions. A phased antenna array enables beamforming by combining multiple antenna elements, where each element can be fed with different phase shifts. By steering the radiation of an antenna to the target, the signal can be delivered with a higher power and a higher signal-to-interference-plus-noise-ratio can be achieved at the receiver. Moreover, less potentially interfering power is emitted towards other radio systems. The concept of antenna arrays with adaptive beampatterns is not new and has its origins in the field of radar. The intensive research on beamforming started in the 1990s. It has been applied to many wireless communication applications for imporving the performance [6].

Beamforming techniques for VHF A/G communications have been investigated in 2008 by Yao Lu, [7], [8]. His work shows an improvement in bit error rate performance. In 2013, multi-antenna systems were studied by Bai [9] and Xie [10] for L-Band A/G communications. They focused on space division multiple access technology in their work to increase spectral efficiency. Lastly, Zhang proposed a two-dimensional circular antenna array layout for a better capacity in aeronautical communications [11]. However, an antenna array design considering its

suitability for LDACS, has not been investigated yet.

The objective of this paper is to analyze the application of beamforming in LDACS. In this study, we consider that the antenna array is located at the ground station (GS) and analyse the benefits of beamforming in the reverse link (RL). The airborne station (AS) uses an omnidirectional antenna as initially proposed for LDACS. We evaluate the beampatterns of different designs and find the most suitable configurations for LDACS. Subsequently, we consider different flight scenarios with a realistic LDACS link budget to calculate the signal-to-noise ratio (SNR) improvement and compare it with the performance of the initially proposed omnidirectional antenna.

The paper is structured as follows: We first discuss the potential challenges. Secondly, the fundamental parameters of antennas are explained. Then, the system model is introduced, state-of-the-art array designs are explained, and their performances assessed. The results are then presented and discussed before concluding the paper.

Challenges of Applying Beamforming in LDACS

This section discusses the possible challenges of applying beamforming in LDACS A/G communications. First of all, LDACS is at a late development stage. The LDACS specification assumes the use of non-steerable antennas. Adjustment in the antenna installation at the GS might require modifications in some LDACS protocols and services as well.

One of the foreseeable problems is going to arise during the cell entry. The entry of an airplane into a cell of a cellular system is always a critical process since, at this point, there is no mutual knowledge between the two communication partners, i.e., the GS and the AS. As the airplane enters into a cell, the AS should listen to all possible forward link frequencies and initiate the communication. If the GS uses an antenna array to receive AS transmissions in the RL, it might fail at hearing signals coming from the new user because it might be only listening signals coming from specific directions, i.e., where the registered users are [12].

In case the GS cannot recognize a new user, the Resource Allocation Authority will not allocate

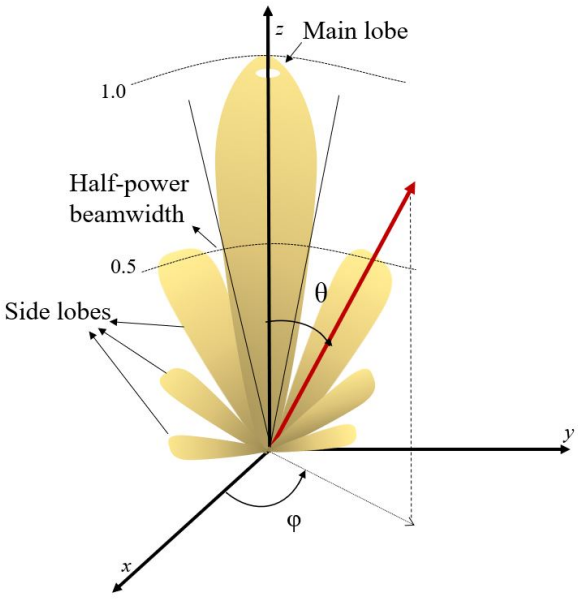

Figure 1. Radiation pattern

required network resources, and it would endanger the safety of flight. In a typical cellular system, the Random Access Channel (RACH) is used to initiate communication between both stations. Therefore, the omnidirectional antenna should be kept at the GS to make sure that the random access message in the RACH can be received by the GS. After the handshake procedure between the AS and GS is completed, the adaptive antenna array can be employed for the rest of the communications.

Fundamental Parameters of Antennas

In this section, definitions of various parameters are explained to describe the performance of antennas. A typical radiation pattern of an antenna is shown in Figure 1 as a polar plot in linear units. The various parts of the radiation pattern can be sub-classified into main and side. The main lobe consists of the direction of maximum radiation. A side lobe is any radiation lobe steered in any direction other than the target. θ denotes the angle between the vertical line and the target, and ϕ denotes the angle between the x-axis and the projection of the target to the ground.

The Half-Power Beamwidth (HPBW) is the angle between two sides of the main beam in which the radiation intensity is one-half the maximum value of the main lobe [13]. The main lobe of the antenna can

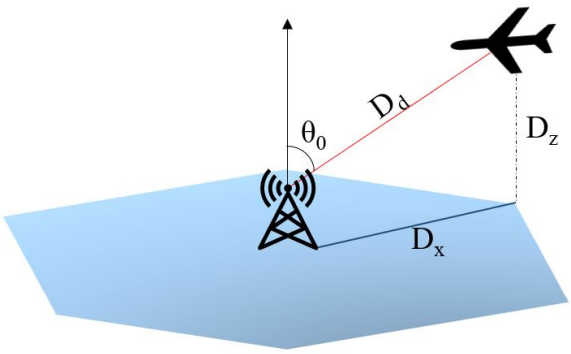

Figure 2. Geometric setup

be focused in both directions, i.e., transmission and reception.

The radiation intensity $U(\theta, \phi)$ is the power radiated from an antenna per unit solid angle. It can be calculated from the far-zone electric field $\mathbf{E}(r, \theta, \phi)$ of an antenna by [13]

$$U(\theta, \phi) = \frac{r^2}{2\eta} |\mathbf{E}(r, \theta, \phi)|^2 \quad (1)$$

where η is the instrinsic impedance of the medium and r is the distance.

The gain $G(\theta, \phi)$ of an antenna can be obtained by [13]

$$G(\theta, \phi) = \frac{e_{cd} U(\theta, \phi)}{U_0} \quad (2)$$

where U_0 denotes the radiation intensity of an isotropic source, and e_{cd} is the antenna efficiency. If the direction of the gain is not given, it implies the direction of the main lobe.

System Model

An omnidirectional antenna and a phased antenna array are placed at the GS for the reception of the RL signal. The omnidirectional antenna will be employed for the RACH; once the handshake procedure is completed, the phased array is used for the communications with the airplane.

Geometry

The geometry of the model is illustrated in Figure 2. D_z denotes the altitude of the airplane, the distance between the airplane and the GS is denoted by D_d, and the distance between the projection of the airplane on the ground to GS is denoted by D_x. θ_0 is the angle between the airplane and an z-axis located at the GS. The cell size is 120 nautical miles (NM), the position of the airplane changes according to the considered scenario.

In case there are multiple airplanes in the cell, the beamforming could be switched between airplanes, or multiple main lobes can be shaped; however, these scenarios have not been addressed in this paper. For simplicity, we first consider a single airplane in the cell.

Scenarios

In this section, we explain three flight scenarios to evaluate the performance of the beamforming approach. In each scenario, the GS steers the main lobe toward the AS as it moves:

- Firstly, we evaluate the performance of the communication when the airplane is furthest away from the GS, i.e., at the border of the cell. The cell border is one of the vulnerable points of A/G communications due to the high path loss between the AS and GS. We analyze the relation between the number of elements in the array and their beamwidths. The trade-off between cost, size, and antenna gain is discussed.
- Secondly, we focus on the angle between the airplane and an z-axis located at the GS, θ_0. The distance in between is kept constant in this scenario. We analyze the difference in antenna gain when the direction of the main beam is varied and the resulting SNR with respect to the different number of elements in the array.
- Lastly, we assume the airplane travels at a constant altitude from the border of the cell to the right above the GS. Thereby, θ_0, D_x, and D_d vary in this scenario. We examine the variation of θ_0 during the flight and its resulting effect on SNR together with the path loss. We compare the results of this case with the use of an omnidirectional antenna for the same flight scenario.

Link Budget

The link budget of the system is calculated according to the LDACS specifications [14]. The only difference is made at the receiver's antenna gain. The LDACS specification assumes an omnidirectional

Table 1. LDACS Link Budget for RL

TX Parameters	
TX output power	42 dB
TX antenna gain	3 dBi
TX cable loss	3 dB
Duplexer loss	1 dB
RX Parameters	
RX cable loss	2 dB
Duplexer loss	0 dB
Total RX noise power	-108.03 dBm

antenna with 12 dBi gain in azimuth direction. Phased arrays are mostly built using patch (microstrip) antennas. An antenna consisting of a single patch typically achieves a gain in the range of 6-9 dBi [15]. In this paper, we assume 7 dBi. Phased arrays with several patches can achieve considerable higher gains than the standard LDACS antenna.

The mid-band frequency for the RL is 987 MHz, the path loss, L_p, is calculated according to

$$L_p = 20\log_{10}\left(\frac{4\pi D_d f}{c}\right) \tag{3}$$

where f is the carrier frequency and c is the speed of light. The rest of the parameters for the link budget calculation are summarized in Table 1.

Antenna Array Design

The overall radiation pattern of an antenna array can be shaped by five characteristics which are [13]:

- the relative pattern of the individual elements
- the geometrical configuration of the overall array (linear, circular, rectangular, spherical, etc.)
- the relative displacement between the elements
- the excitation phase of the individual elements
- the excitation amplitude of the individual elements

The total electric field $\mathbf{E}_t$ of the array is equal to the electric field of a single element $\mathbf{E}_s$ multiplied by the array factor (AF) [13]:

$$\mathbf{E}_t = \mathbf{E}_s \mathrm{AF} \tag{4}$$

The gain of the antenna array is calculated using (1) and (2). In this paper, the radiation pattern of a single element is defined according to the cosine exponent law, also called the cosine pattern. It is a close estimation of a realistic patch antenna pattern [16]. Moreover, the radiation pattern of a rectangular planar array is evaluated in the following sections (see Figure 3). The AF for a planar array is [13]

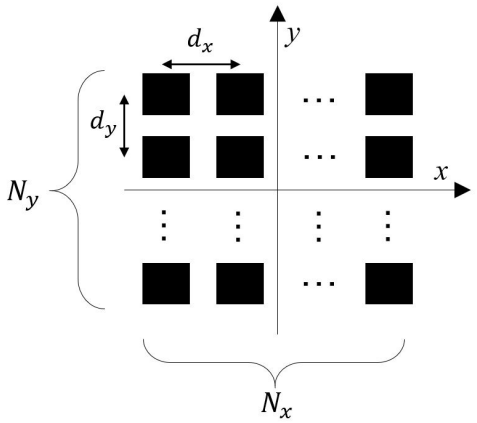

Figure 3. Rectangular planar antenna array

$$\mathrm{AF}(\theta,\phi) = \sum_{m=1}^{N_x}\sum_{n=1}^{N_y} w_{mn} e^{j[(m-1)kd_x \sin\theta\cos\phi + (n-1)kd_y \sin\theta\sin\phi]} \tag{5}$$

where $k = 2\pi/\lambda$ is the wavenumber, λ is the carrier wavelength, and w_{mn} is the amplitude excitation of each element. N_x denotes the antennas in each row and N_y antennas in each column. In this paper, we consider the number of elements in each row equal to in each column $N_x = N_y = N$. The antenna elements are separated by $d_x = d_y = \lambda/2$ to decrease the mutual coupling between the elements. A larger separation would cause unwanted beams with a high directivity, so called grating lobes [16].

The main lobe can be steered in different directions by controlling the phase excitation difference, β, between the antenna elements. In order to orientate the maximum beam to (θ_0, ϕ_0) where $0° \leq \theta_0, \phi_0 \leq 180°$, the phase excitation difference between the elements needs to be as follows [13]:

$$\beta_{mn} = -k(x_m \sin\theta_0\cos\phi_0 + y_n \sin\theta_0 \sin\phi_0) \tag{6}$$

The proper amplitude distribution (tapering) from the middle to the side can be used to control the beamwidth and side lobe. The smoother the taper from the center of the array toward the edges, the lower the side lobe level and larger the beamwidth. On the contrary, when the amplitude distribution is abrupt, it results in the highest side lobe level with the narrowest beamwidth [13].

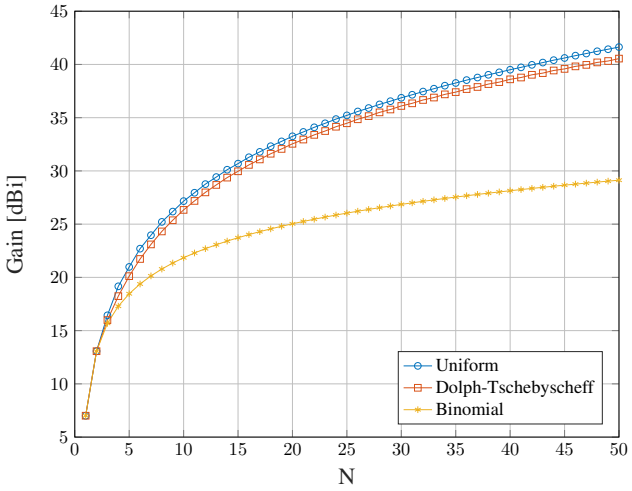

Figure 4. Gain of the NxN antenna array

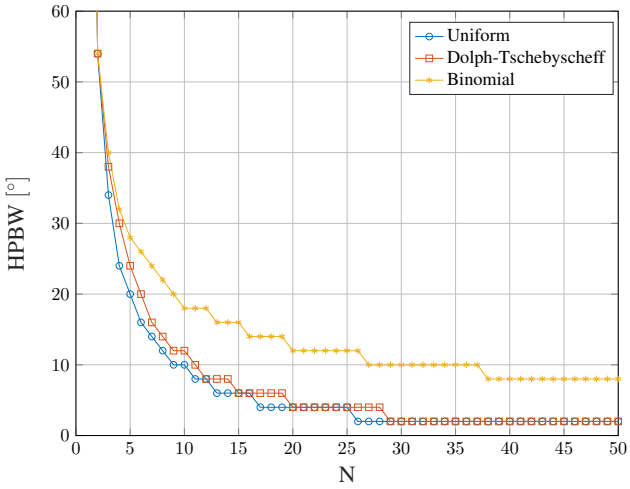

Figure 5. HPBW of the NxN antenna array

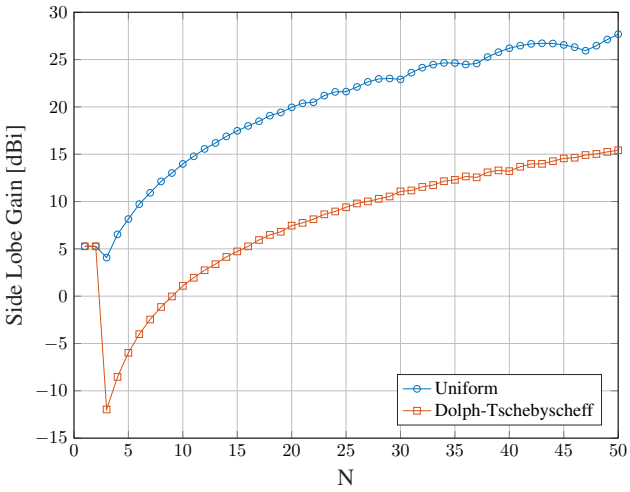

Figure 6. Side lobe level of the NxN antenna array

Assessment of Array Designs

This section evaluates and compares beampatterns of the different array designs. The performance of each design is assessed considering the maximum gain, side lobe level, and HPBW. Firstly, different amplitude distributions are assessed for the changing number of antenna elements at each edge. Secondly, antenna arrays are steered in different directions, and alterations in radiation patterns for varying θ_0 are analyzed.

Three typical amplitude distributions have been evaluated in this paper: uniform, Dolph-Tschebyscheff, and binomial. In uniform arrays, all elements have equal amplitude excitations. In binomial and Dolph-Tschebyscheff arrays, amplitude excitations are derived from the binomial expansion and Dolph-Tschebyscheff polynomials, respectively [13]. For the Dolph-Tschebyscheff array, the main to minor lobe intensity ratio (R_0) is set to 25 dB.

Amplitude Excitation

The maximum gain, side lobe level, and HPBW of the three distributions are calculated for varying antenna numbers in the range of 1 to 50 elements on each edge. For $N \leq 2$, all arrays have the same amplitude distribution, thereby the same radiation pattern. As it is plotted in Figure 4 and 5, the uniform array achieves the highest gain and narrowest beamwidth, followed by the Dolph-Tschebyscheff and binomial arrays.

The beamwidth of the antenna is essential to direct the signal in the intended direction and to avoid interferences of the undesired signals coming from other directions. The narrower the beamwidth, the higher the gain of the main lobe. However, shaping a too narrow beamwidth might also bring some disadvantages to A/G communications. First of all, the GS will have to track the AS with a high accuracy to ensure that the signal is directed to the target. Secondly, a narrower main lobe means fewer aircraft will be located in that direction. Hence, fewer aircraft will be able to benefit from the high gain communication simultaneously, and the main beam will be needed to be switched more often between aircraft. Therefore, the beamwidth should be compromised in a way that it can steer to a certain number of aircraft at once.

The ratio between the main lobe and side lobe

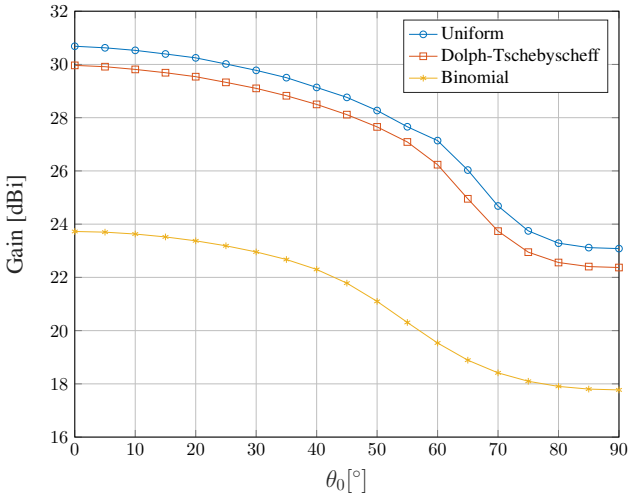

Figure 7. Gain vs. θ_0 for 15x15 antenna array

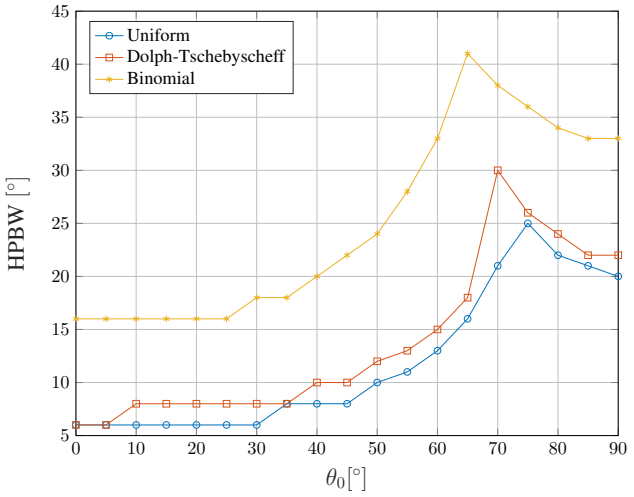

Figure 8. HPBW vs. θ_0 for 15x15 antenna array

is essential for understanding how well the power is directed in the intended direction [13]. Figure 6 demonstrates that Dolph-Tschebyscheff array accomplishes lower side lobe levels than the uniform array, while the binomial array achieves no side lobes. Nevertheless, it is impractical to use binomial arrays due to large amplitude variations among the elements. It is also an inefficient design because the magnitude of the extreme elements is negligible compared to those toward the center. As a result, Dolph-Tschebyscheff is a compromise design that can achieve a low side lobe level, a narrow beamwidth, and a high gain.

Phase Excitation

Considering the increment at the gain regarding the number of antenna elements, the evaluation of the steering capability is decided to be done for $N_x = N_y = N = 15$.

The gain and HPBW of the array designs are calculated for $\phi_0 = \pi/2$ and $0^\circ \leq \theta_0 \leq 90^\circ$. As it can be seen in Figure 7 and 8, as θ_0 increases, the gain decreases and the beamwidth of the main lobe widens. The change in the radiation pattern is due to scanning loss: an increase in θ_0 causes a reduction in the sensitivity of the array [16]. This effect widens the beamwidth accordingly. In Figure 8, the decrease in the beamwidth after a certain θ_0 value is because the beam is too close to the horizontal line and the ground cuts a part of it.

Results

After evaluating the radiation patterns of the antenna array designs, we consider the Dolph-Tschebyscheff array for the realistic LDACS communications scenario. Since the directivity of the array does not enhance significantly for $N \geq 20$, we consider up to 20 elements at each edge.

The first scenario analyzes the performance of the array with respect to the SNR and the beamwidth when the airplane is at the border of the cell. The altitude of the airplane is $D_z = 10$ km and the angle between the airplane and the GS is $\theta_0 = 87^\circ$. In Figure 9, we evaluate the SNR for varying number of antenna elements and compare it with the SNR of the current LDACS implementation. For $N < 3$, the current LDACS provides a better SNR. The reason is that the gain of the LDACS receiver antenna is 12 dBi. In comparison, the gain of a single patch antenna is assumend to be 7 dBi. The gain of the phased antenna array increases as the number of patch antenna elements increases. According to the results, the array should have at least 3x3 antenna elements to be able to improve the performance of of LDACS as assumed in its specification. Moreover, the SNR increases logarithmically as the number of elements at each edge increases. However, adding another antenna element to each edge of the array increases the number of elements exponentially since the number of antenna elements equals N^2. More antenna elements also mean a larger array size and a higher cost. In Figure 10, we evaluate the HPBW

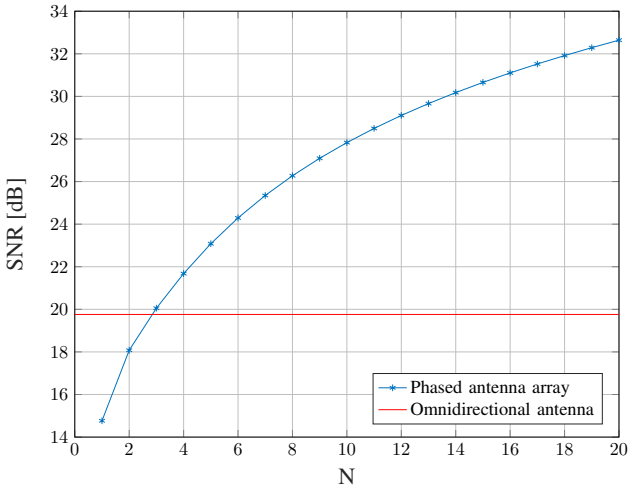

Figure 9. SNR for NxN antenna array vs. omni-directional antenna

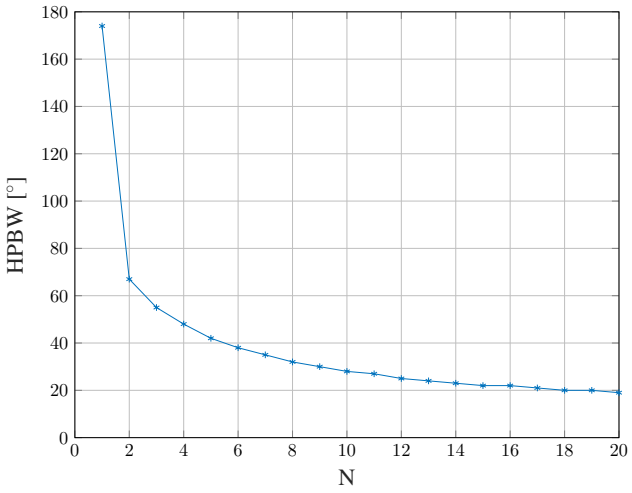

Figure 10. HPBW for NxN antenna array

of the antenna arrays when the airplane is at the border of the cell. For $N \geq 12$, we observe that the beamwidth does not significantly decrease anymore. The second scenario focuses on the angle θ_0 between the airplane and the antenna array for a constant distance in between. This scenario is evaluated for $N \in \{5, 10, 15, 20\}$. In Figure 11, we observe the beam broadening effect. As θ_0 increases, the SNR decreases and the beamwidth widens. In Table 2, for each N value, the SNR for $\theta_0 \in \{0, 90\}$ and the difference between them, the SNR range, are given. The SNR range increases for larger arrays. Therefore, incrementing the number of antenna elements leads to more drastic variations in the SNR as the θ_0 changes. In Table 2, we also see that the SNR difference for

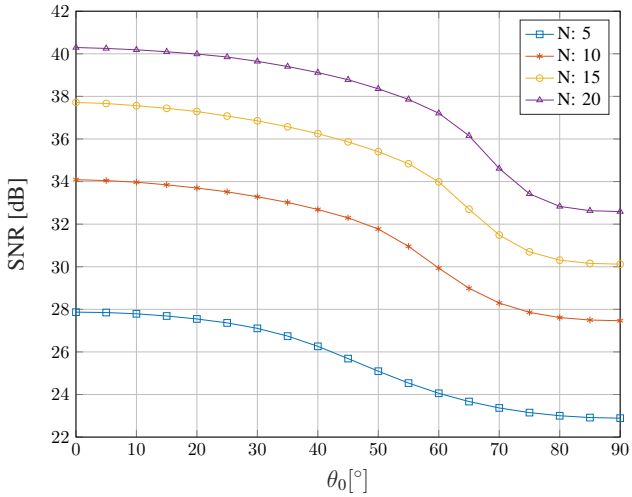

Figure 11. SNR vs. θ_0 for NxN antenna array

Table 2. SNR vs. θ_0

N	SNR [dB]		SNR range [dB]	Antenna size [m^2]
	$\theta_0 = 0°$	$\theta_0 = 90°$		
5	27.87	22.89	4.98	0.61^2
10	34.09	27.47	6.62	1.36^2
15	37.72	30.12	7.59	2.13^2
20	40.3	32.59	7.70	2.88^2

$N = 10$ and $N = 15$ is approximately 3 dB. In other words, the signal power doubles, and the number of antenna elements increments by 125 from 10x10 to 15x15. The SNR difference for $N = 15$ and $N = 20$ is approximately 2.5 dB, where the number of antenna elements increases by 175, from 15x15 to 20x20. However, according to Figure 10, both $N = 15$ and $N = 20$ provide the same beamwidth at the border of the cell. To sum up, considering the results of the first two scenarios, 15 antenna elements at each edge of the antenna array suggest a good compromise for the performance, i.e., 225 antenna elements and 2.13 m x 2.13 m antenna size.

In the last scenario, the airplane travels at a 10 km altitude from the border to the center of the cell. This time, both θ_0 and D_x are changed (see Figure 2). This scenario is evaluated for $N = 15$. In Figure 12, the left vertical axis shows the SNR and the right vertical axis shows θ_0 with respect to D_x. In 82% of the path, $\theta_0 \in [77, 87]$. In Figure 11, it is shown that for $N = 15$ and $75° \leq \theta_0 \leq 87°$, the SNR only slightly alters. Therefore, the variation in the SNR during the airplane's travel is mostly due

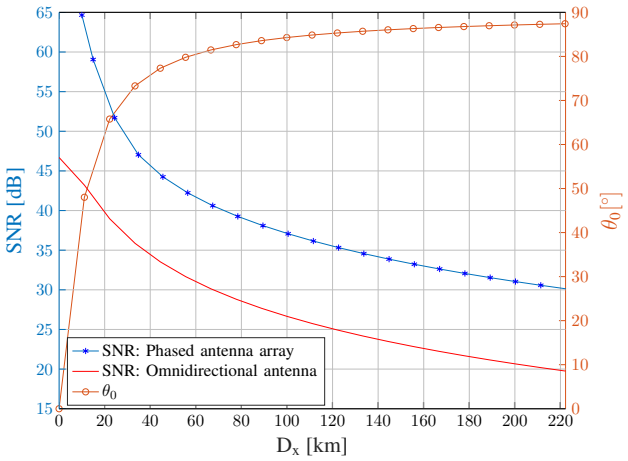

Figure 12. SNR and θ_0 vs. D_x

to the change in the path loss, which is the same when using an omnidirectional antenna. As a result, the SNR is improved for the entire path compared to the antenna assumed in the LDACS specification. In 82% percent of the path, the phased antenna array with $N = 15$ improves the SNR by approximately 10 dB compared to the antenna assumed in the LDACS specification. In the rest of the path, when $D_x \leq 40$ km, θ_0 decreases dramatically. Therefore, the gain of the antenna array increases abruptly (see Figure 11). Consequently, the SNR increases even further, above 20 dB. This increment in the SNR enhances the robustness of the LDACS physical layer and enables it to achieve higher data rates by using its adaptive coding and modulation capability.

Conclusion

In this paper, we investigate applying beamforming in the LDACS RL to enhance the reception at the LDACS GS. We first discuss possible challenges and assess different antenna array designs considering their radiation pattern. Accordingly, the most suitable antenna array design is evaluated in different scenarios of interest for LDACS A/G communications. It is shown that by using a 15x15 Dolph-Tschebyscheff antenna array, the SNR in the RL can be increased by over 10 dB. Hence, beamforming can improve the robustness of the physical layer and enable the system to achieve higher data rates by applying the built-in LDACS adaptive coding and modulation capabilities. Moreover, it is shown that a phased antenna array can achieve a narrower beamwidth compared to an omnidirectional antenna. Thus, any interference coming from other directions is less likely to affect LDACS communications. In our future work, we will evaluate the increase in data rate achievable by using beamforming combined with adaptive coding and modulation for LDACS.

References

[1] "Challenges of Growth, Task 4: European AirTraffic in 2035," EUROCONTROL, Tech. Rep., 06 2013. [Online]. Available: http://www.eurocontrol.int/statfor

[2] SESAR, homepage = http://www.sesarju.eu.

[3] NextGen, homepage = http://www.faa.gov/nextgen.

[4] M. Schnell, U. Epple, D. Shutin, and N. Schneckenburger, "Ldacs: future aeronautical communications for air-traffic management," *IEEE Communications Magazine*, vol. 52, no. 5, pp. 104–110, 2014.

[5] J. Grimes, "Commercial wireless metropolitan area network (wman) systems and technologies," *Memo 8–39*, 2009.

[6] J. Mietzner, R. Schober, L. Lampe, W. H. Gerstacker, and P. A. Hoeher, "Multiple-antenna techniques for wireless communications - a comprehensive literature survey," *IEEE Communications Surveys Tutorials*, vol. 11, no. 2, pp. 87–105, 2009.

[7] Y. Lu, J. An, and Y. Wu, "A differential mimo-beamforming scheme for transmission over aeronautical channels," in *2008 4th International Conference on Wireless Communications, Networking and Mobile Computing*, 2008, pp. 1–4.

[8] Y. Lu and J. An, "A type of adaptive beamforming for self-interference cancellation over aeronautical channel," in *2008 4th International Conference on Wireless Communications, Networking and Mobile Computing*, 2008, pp. 1–4.

[9] L. Bai, J. Xie, W. Guan, and Q. Yu, "A primary rate guaranteed sdma for aeronautical communications," in *2013 8th International Conference on Communications and Networking in China (CHINACOM)*, 2013, pp. 925–929.

[10] J. Xie, L. Bai, and J. Zhang, "Dual priority sdma in aeronautical communications," in *2013 Integrated Communications, Navigation and Surveillance Conference (ICNS)*, 2013, pp. 1–9.

[11] C. Zhang and K. Pang, "Two-dimensional circle antenna layout for aeronautical mimo communications," *IEEE Antennas and Wireless Propagation Letters*, vol. 12, pp. 1566–1569, 2013.

[12] D. M. Mielke, "Circumventing the random access

channel: New concepts for accessing a command amp; control link for unmanned aircraft," in *2019 IEEE/AIAA 38th Digital Avionics Systems Conference (DASC)*, 2019, pp. 1–6.

[13] C. A. Balanis, *Antenna theory: analysis and design*. Wiley-Interscience, 2005.

[14] EECNS, "SESAR2020 PJ14-02-01 - LDACS A/G Specification," SESAR Joint Undertaking, Tech. Rep., 2019.

[15] A. Rivera-Albino and C. A. Balanis, "Gain enhancement in microstrip patch antennas using ferrite rings," in *2013 USNC-URSI Radio Science Meeting (Joint with AP-S Symposium)*, 2013, pp. 228–228.

[16] R. Mailloux, "Phased array theory and technology," *Proceedings of the IEEE*, vol. 70, no. 3, pp. 246–291, 1982.

Acknowledgements

We would like to thank Dr. Stefano Caizzone and Federico Boulos from the German Aerospace Center (DLR) for sharing their expertise in antenna systems and providing the antenna simulation software.